Current Theoretical Models and High Resolution Solar Observations: Preparing for ATST
ASP Conference Series, Vol. 286, 2003
A. A. Pevtsov and H. Uitenbroek, eds.

Convective Mechanism for Formation of Solar Magnetic Bipoles

A.V. Getling and I.L. Ovchinnikov

Institute of Nuclear Physics, Lomonosov Moscow State University, 117234 Moscow, Russia; A.Getling@ru.net

Abstract. A mechanism for the formation of bipolar magnetic configurations, alternative to the well-known rising-tube mechanism, is considered. In contrast to the latter, it does not require any originally present flux tube of strong magnetic field and ensures *in situ* amplification and structuring of the magnetic field. Cellular magnetoconvection in a plane horizontal layer of an electrically conducting fluid heated from below is simulated numerically within the framework of a fully nonlinear, three-dimensional problem. The initial magnetic field is assumed to be fairly weak and directed horizontally. The initial conditions for velocity specify a pattern of small-amplitude hexagonal cells. It is shown that a hexagonal convection cell can substantially amplify the magnetic field and impart bipolar configurations to it. Depending on the parameters, the amplified field may have the form of either a simple pair of magnetic islands, opposite in polarity, or a more complex superposition of bipoles. In particular, very compact magnetic elements of strong field can form. The resulting pattern of magnetic-field evolution is in better agreement with observations than the rising-tube model.

1. Introduction

This study traces back to the mid-1960s, when Tverskoy (1966) suggested a convective mechanism capable of forming the magnetic fields of bipolar sunspot groups, alternative to the well-known rising-tube mechanism. Tverskoy considered a simple kinematic model, representing a convection cell by a toroidal eddy in a perfectly conducting fluid, and found that convection can produce bipolar configurations of the amplified magnetic field, like those typical of sunspot groups. The original presence of a flux tube of strong magnetic field is not needed for this process, and the topology of the actually observed flows is, on its own, responsible for the basic property of the considered mechanism. As we will see (and as noted by Getling 2001), the pattern of the magnetic-field evolution controlled by this mechanism much better agrees with observations (Bumba 1967) than the rising-tube scenario does.

A comprehensive study of the convective mechanism and a quantitative verification of its efficiency under the solar conditions require numerical simulations of the evolution of three-dimensional flows and magnetic fields based on the full system of MHD equations. Some results of such simulations were reported by

Getling (2001). We present here further developments of this study. At this stage of investigation, we restrict ourselves to a Boussinesq approximation (see, e.g., Getling 1998). In other words, we assume density variations to be negligible small in all terms in the equations except for the term proportional to the gravitational acceleration.

2. Formulation of Problem of Nonlinear Numerical Simulation

We will solve the system of magnetohydrodynamic equations in a Boussinesq approximation for a plane horizontal layer $0 < z < d$ of a fluid with finite electrical conductivity, heated from below. Imagine that the layer under study is bounded from below and above by slabs of a motionless material, perfectly electrically and thermally conductive, and that the lower and the upper boundary are kept at constant temperatures T_1 and T_2, respectively, so that $T_1 - T_2 = \Delta T$. We represent any variable f in the problem as the sum of its *unperturbed* value f_0, which corresponds to the motionless state of the fluid, and a *perturbation*, which is produced by the flow (and, in general, can even substantially exceed the unperturbed value). Let the unperturbed (initial) magnetic field H_0 be uniform and directed horizontally, along the x axis and let h be the magnetic-field perturbation measured in units of H_0. The perturbation of the temperature—i.e., its departure from the linear equilibrium profile $T_0 = T_1 - \Delta T(z/d)$, expressed in units of ΔT—will be designated as θ. We choose d as the unit length and the characteristic time $t_\nu = d^2/\nu$ for viscous dissipation on the scale d as the unit time (here, ν is the kinematic viscosity) and denote the vector of non-dimensional velocity as $\mathbf{u}$.

We write the original system of equations in the following non-dimensional form:

$$\frac{\partial \mathbf{u}}{\partial t} + (\mathbf{u}\cdot\nabla)\,\mathbf{u} = -\nabla\varpi + \frac{R}{P_1}\hat{\mathbf{z}}\theta - \frac{Q}{P_2}(\hat{\mathbf{H}}_0 \times [\nabla\times\mathbf{h}] + \mathbf{h}\times[\nabla\times\mathbf{h}]) + \Delta\mathbf{u}, \tag{1}$$

$$\frac{\partial \mathbf{h}}{\partial t} = \nabla\times[\mathbf{u}\times\hat{\mathbf{H}}_0] + \nabla\times[\mathbf{u}\times\mathbf{h}] + \frac{1}{P_2}\Delta\mathbf{h}, \tag{2}$$

$$\frac{\partial \theta}{\partial t} - u_z + (\mathbf{u}\cdot\nabla)\,\theta = \frac{1}{P_1}\Delta\theta, \tag{3}$$

$$\nabla\cdot\mathbf{u} = 0, \tag{4}$$

$$\nabla\cdot\mathbf{h} = 0. \tag{5}$$

Here, $\hat{\mathbf{H}}_0 = \mathbf{H}_0/H_0$, and $\hat{\mathbf{z}}$ is a unit vector directed along the z coordinate axis, vertically upward. The quantity ϖ is the non-dimensional form of the combination p'/ρ_0 (where p' is the pressure perturbation and ρ_0 is the density at temperature T_0). The non-dimensional parameters

$$R = \frac{\alpha g\,\Delta T\,d^3}{\nu\chi}, \quad Q = \frac{H_0^2 d^2}{4\pi\rho_0\nu\nu_\mathrm{m}} = \frac{H_0^2 d^2\sigma}{\rho_0 c^2\nu}, \quad P_1 = \frac{\nu}{\chi}, \quad P_2 = \frac{\nu}{\nu_\mathrm{m}} = \frac{4\pi\sigma\nu}{c^2} \tag{6}$$

(where α is the volumetric thermal-expansion coefficient of the fluid, χ its thermal diffusivity, σ its electrical conductivity, and ν_m its magnetic viscosity) are

the Rayleigh number, Chandrasekhar number, normal Prandtl number, and magnetic Prandtl number, respectively. They are the basic parameters of the problem. In addition, given the shape and orientation of the originally present convection cells, the magnetic-field evolution depends on their size (i.e., on the initially specified flow wavenumber).

We assume the surfaces of the layer to be free-slip and impermeable; i.e., we specify the condition that the normal (vertical) velocity component and tangential stresses vanish at these surfaces:

$$u_z = \frac{\partial u_x}{\partial z} = \frac{\partial u_y}{\partial z} = 0 \quad \text{at} \quad z = 0,\ 1. \tag{7}$$

If the slabs bounding the layer are perfectly electrically conducting, the boundary conditions for the magnetic field have a quite similar form:

$$h_z = \frac{\partial h_x}{\partial z} = \frac{\partial h_y}{\partial z} = 0 \quad \text{at} \quad z = 0,\ 1. \tag{8}$$

In our formulation of the problem, the temperature perturbations vanish at the layer boundaries:

$$\theta = 0 \quad \text{at} \quad z = 0,\ 1. \tag{9}$$

We employ a Galerkin (spectral) technique, assuming the velocity, magnetic field, and thermal perturbation to be periodic functions of the coordinates x and y. We introduce spectral representations of these functions in the form of partial sums of trigonometric Fourier series; the boundary conditions (7)–(9) also make it possible to choose trigonometric functions to describe the z dependences.

The number of harmonics used in our computations was 64^3 or 32^3 (including the zero harmonics). To reduce the number of variables, we restricted our consideration to physical fields with a certain symmetry with respect to the coordinate origin (see Figs. 1, 3 below); in this case, the spectral coefficients (harmonic amplitudes) obey certain parity relations in their indices corresponding to the x and y dependences.

The substitution of the spectral representations into the original system (1)–(5) reduces it to a system of ordinary differential equations for the amplitudes of harmonics as functions of time. We use a fast Fourier transform procedure to calculate the convolution sums in the right-hand sides of the spectral equations, and employ a fourth-order Runge–Kutta method to carry out the integration over time.

3. Results

In each run, a weak initial perturbation of the motionless state of the fluid was specified in the form of an x- and y-periodic pattern of Bénard-type hexagonal cells (Fig. 1a); viz.,

$$u_z = -4\frac{A}{\pi}\left(2\cos\sqrt{3}\beta x\,\cos\beta y + \cos 2\beta y\right)\cos\pi z \quad \text{at} \quad t = 0, \tag{10}$$

where $A = -0.1$ [with the corresponding expressions for u_x and u_y according to (4)]. Thus, the fundamental wavenumber of the pattern $k_0 = 2\beta$ was defined.

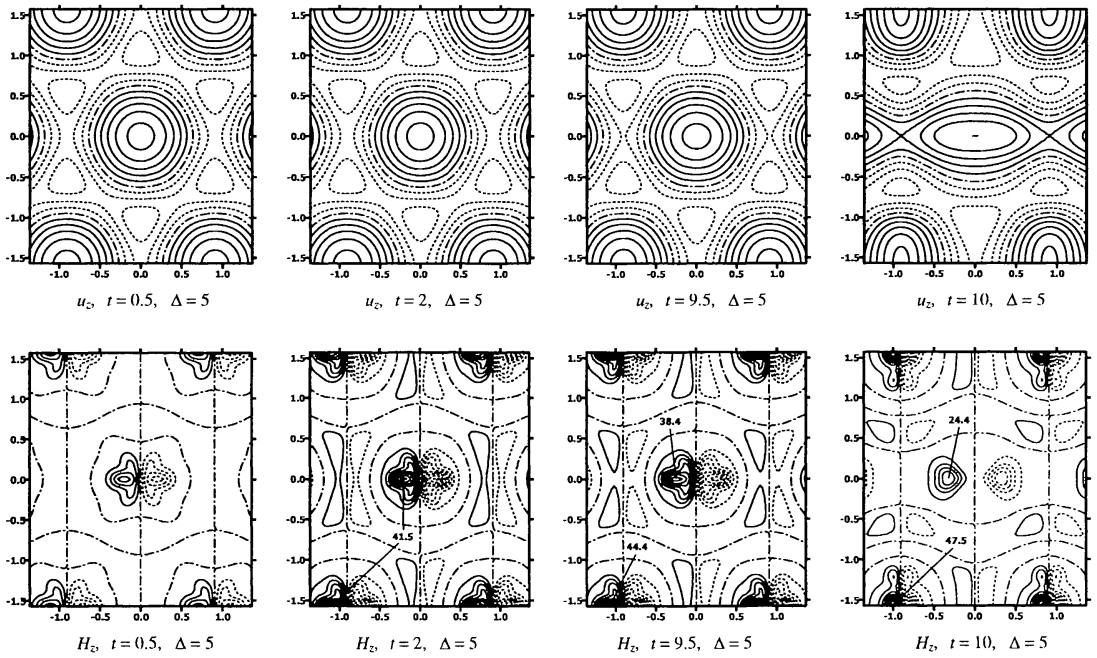

Figure 1. Evolution of the flow (top) and magnetic field (bottom) for $R = 3000 = 4.56R_c$, $P_1 = 1$, $P_2 = 10$, $Q = 0.01$, $k_0 = 4 = 1.8k_c$ ($R_c = 657.5$ is the critical Rayleigh number at which convection sets in, and k_c is the critical wavenumber). Contours of the vertical components of the velocity, u_z, and magnetic filed, H_z, in the midplane $z = 1/2$ of the layer are shown with contour increment Δ.

If the distribution of the material parameters of the fluid over the layer does not exhibit any significant asymmetry with respect to the midplane $z = 1/2$, convection most typically assumes the form of two-dimensional rolls, while hexagonal convection cells are in many cases unstable. An externally imposed horizontal magnetic field also favors the transformation of hexagons into rolls aligned with this field (Chandrasekhar 1961). After such a transformation, the magnetic field can no longer be amplified. Thus, for the formation of a three-dimensional configuration of the amplified field, the initial field must not be too strong, so that a substantial amplification be possible before the transition to the roll flow. In all scenarios computed, a transition to rolls ultimately took place. We will not discuss here the relevance of this effect to solar magnetoconvection and will only be interested in that stage of the process when the flow is three-dimensional.

We will describe here two scenarios of the flow and magnetic field evolution. The first one corresponds to moderate values of R and P_2 and a fairly small value of Q (Figs. 1, 2). It can be called the *basis* scenario, since its main features are typical of regimes with a "quiet" development of the process and a relatively simple magnetic field structure. Crudely, by the time $t = 0.5$, the cellular flow settles down to a steady state, which persists almost until $t = 9$. During the interval $0 < t < 2$, the magnetic field is amplified by the flow (the *growth stage*), and characteristically bipolar configurations—pairs of compact

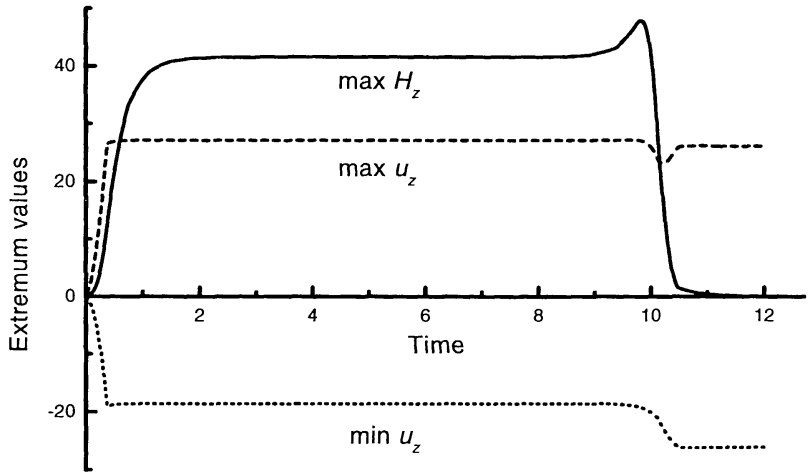

Figure 2. Time variation of extremum values of the vertical components of the magnetic field and velocity for $R = 3000 = 4.56R_c$, $P_1 = 1$, $P_2 = 10$, $Q = 0.01$, $k_0 = 4 = 1.8k_c$.

magnetic islands—develop in the zones of convective upwelling, near the cell centers. By $t = 2$ or so, a *steady-state stage* comes, with a magnetic-field strength of about 41.5 (in units of H_0) within the islands. The magnetic islands remain nearly identical in all upwellings as long as the velocity field retains its original symmetry. Between $t = 8$ and 9, a transition to a two-dimensional roll flow begins. For the given initial conditions (with the given fundamental wavenumber), the upwellings located at $y = \pm\pi/2, \pm 3\pi/2, \ldots$ are compressed by the interspacing downwellings, and the magnetic field in these upwelling regions is additionally amplified (the *compression stage*). At the same time, the upwellings located at $x = 0, \pm\pi, 2\pm\pi, \ldots$ merge, and the magnetic field weakens there. The magnetic-field compression is reflected by the peak in the curve of $\max H_z$ in Fig. 2 near $t = 9.9$, whose height is 49.1. Ultimately, the magnetic-field *decay stage* results in the recovery of the initial field, with a simultaneous formation of a roll flow.

The second scenario (Figs. 3, 4) is characterized by larger R, P_2, and Q; in addition, the fundamental wavenumber is equal to the critical one. The evolution is more complex in this case, without a steady-state stage in the variation of the magnetic field. Because of the different k_0, the transition to rolls does not involve a compression of upwellings, and the corresponding stage in the magnetic-field evolution is also missing. During the decay stage, the amplified magnetic field is fragmented, and its remnants survive relatively long. As a result, an apparently non monotonic behavior of $\max H_z$ and $\max u_z$ can be noted. The most interesting feature of this scenario is the formation, in a convection cell, of a pair of very small magnetic elements with a high magnetic-flux concentration. These elements grow rapidly and reach a wide spatial separation very early. A significant magnetic-flux concentration at the peripheries of the cells can be noted.

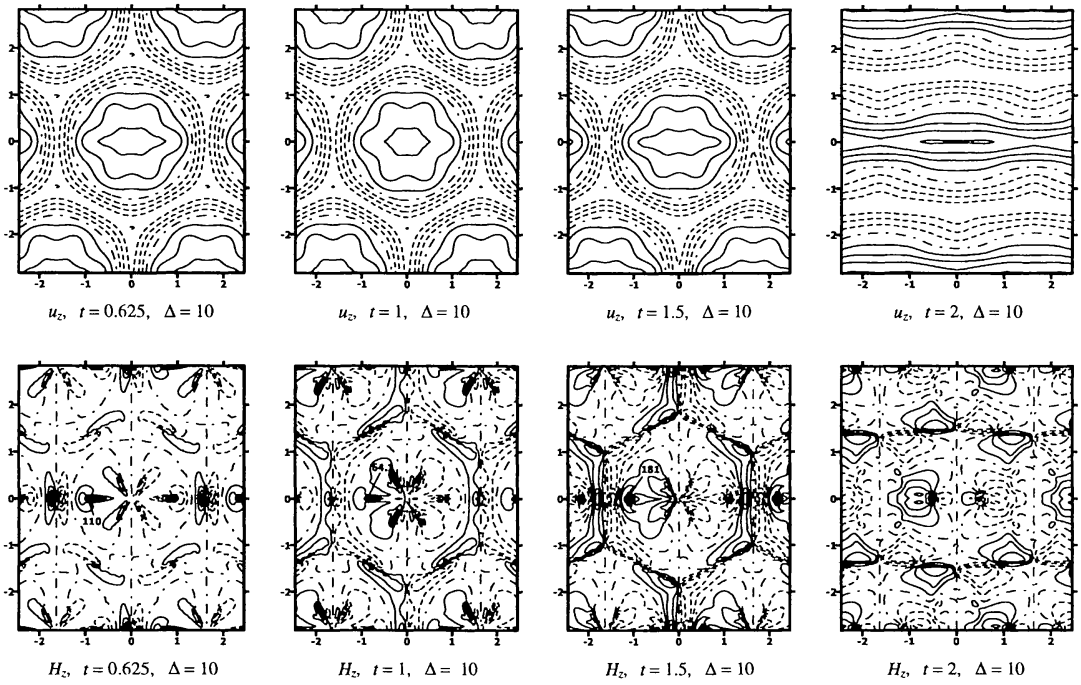

Figure 3. Same as in Fig. 1 but for $R = 5000 = 7.6R_c$, $P_1 = 1$, $P_2 = 30$, $Q = 1$, $k_0 = 2.22 = k_c$.

In any particular case, the efficiency of the convective mechanism can be measured by the maximum achieved non-dimensional H_z and the ratio γ of the maximum values of the magnetic- and kinetic-energy densities E_m and E_k:

$$E_m = \frac{H_0^2\,(\max H_z)^2}{8\pi}, \quad E_k = \frac{\rho_0\,(\max u_z)^2}{2}\frac{\nu^2}{d^2}, \quad \gamma = \frac{E_m}{E_k} = \frac{Q\,(\max H_z)^2}{P_2\,(\max u_z)^2}. \quad (11)$$

This ratio increases with R and P_2, and also, within certain range, with Q. At Q exceeding some limit, the flow is strongly braked by the magnetic field, and high $\max H_z$ cannot be achieved. In the first scenario described here, H_z reaches 49.1 near $t = 9.9$. At this instant, $\gamma = 0.003$. However, increasing R to 5000 and Q to 1 yields, at the compression stage, an H_z maximum of 78 and a γ maximum of 0.44. The second scenario yields main-peak values of $\max H_z = 181.3$ and $\gamma = 2$ at $t = 1.47$. At the first $\max H_z$ peak ($t = 0.625$), these quantities are 109.9 and 0.74, respectively.

4. Discussion

Thus, our computations confirm the qualitative predictions based on the model of Tverskoy (1966). The above-described convective mechanism of magnetic-field amplification and structuring can be very efficient and is promising in the context of searches for sources of strong photospheric magnetic fields. In particular, our computations demonstrate the possibility of the formation of very compact magnetic islands. For this reason, it will be useful to investigate the possible

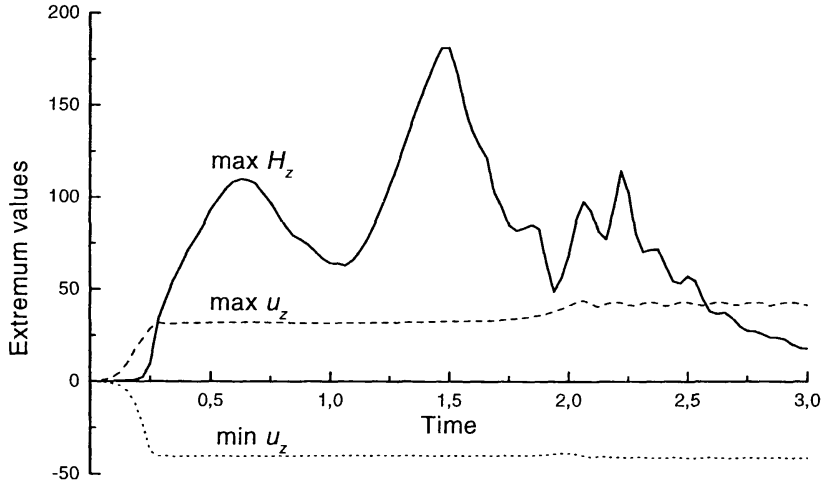

Figure 4. Same as in Fig. 2 but for $R = 5000 = 7.6R_c$, $P_1 = 1$, $P_2 = 30$, $Q = 1$ $k_0 = 2.22 = k_c$.

role of this mechanism in producing not only sunspots and active regions, but also small-scale magnetic elements.

At this stage, it would be premature to attempt to estimate the parameter values typical of the solar convection zone, where the viscosity and thermal conductivity are controlled by turbulent transport and are thus highly indeterminate. Large Rayleigh numbers R can be expected; however, the mere presence of a relatively regular supergranular pattern on the Sun suggests that the effective R for the corresponding layers is maintained by small-scale turbulent processes on a level for which convection remains quasi-laminar. The electrical conductivity of the solar plasma in the convection zone grows rapidly with depth, reaching values for which the magnetic field can be considered to be completely frozen in the plasma. Turbulence should reduce the effective conductivity. Nevertheless, as can be judged by the observed picture, the magnetic-field dynamics do not depart too strongly from a freezing-in regime, even in layers that can be directly observed; therefore, the magnetic Prandtl number P_2 still remains fairly high. Effective hydrodynamic Prandtl numbers of order unity are considered to be plausible.

This mechanism can operate on various spatial scales, since its main properties are determined by the flow topology. While regular supergranular cells may be responsible for the formation of small magnetic elements, an especially large and intense cell, which encompasses layers deeper than usual and which is threaded with a weak seed magnetic field, could produce the magnetic fields of sunspot groups. Diverse initial conditions can ensure the generation of diverse configurations of the amplified magnetic field—superpositions of unipolar, bipolar, and higher multipolar fields. If the seed field threads a group of cells, the interaction of the flows with the magnetic field will be "collective," and the amplified field will have an even more complex structure. The seed field is unlikely to be highly ordered, but the spatially averaged vector of this field could naturally be identified with the large-scale toroidal (latitudinally directed) mag-

netic field; the initial presence of this preferred direction of the magnetic field is, in principle, sufficient for the field to subsequently evolve in qualitative agreement with the computed scenarios. The seed toroidal field should be controlled by large-scale dynamo processes and should thus introduce a global regularity into the distribution of sunspot groups. The magnetic bipoles produced by this mechanism obey the Hale law of magnetic polarities. Nothing but convection on supergranular and sunspot scales would serve as a connecting link between the global and local processes.

To **summarize,** we note the following. The convective mechanism considered here, which does not require strong initial magnetic fields, can form bipolar (and multipolar) configurations of a strongly amplified magnetic field on various spatial scales. It provides a natural explanation for the general, global regularities in the behavior of local solar magnetic fields. The above-presented notion of the magnetic-field amplification process is free of the contradictions with observations that are inherent in the rising-tube model:

(1) If a tube of a strong magnetic field emerges, it will completely break down the pre-existing convective velocity field. In contrast, the actually observed flow pattern normally remains virtually intact in the process of local magnetic-field growth; the magnetic field only gradually *seeps* through the photosphere, remaining in conformity with the velocity field (Bumba 1967). It is such a situation that should take place if the magnetic field is produced by the convective mechanism.

(2) Such dramatic effects of the tube emergence as plasma streams spreading from the site above the rising tube should be especially impressive but have never been observed. They are not implied by the convective mechanism.

(3) The emerging magnetic field itself, strong and mainly horizontal, would be directly observed in the photosphere as one of the most prominent features of the process, but nothing of the sort actually takes place. If the convective mechanism operates, similar effects should not be expected.

Acknowledgments. We are grateful to the Pushchino Radio Astronomy Observatory of the Russian Academy of Sciences for the availability of computer resources and to L. M. Alekseeva for perpetual fruitful discussions. This work was supported by the Russian Foundation for Basic Research (project code 00-02-16313).

References

Bumba, V. 1967, in Rendiconti della Scuola Internazionale di Fisica "E. Fermi", 39 Corso, 77

Chandrasekhar, S. 1961, Hydrodynamic and Hydromagnetic Stability (Oxford: Clarendon Press)

Getling, A. V. 1998, Rayleigh–Bénard Convection: Structures and Dynamics (World Scientific, Singapore); Russian version: 1999 (URSS, Moscow)

Getling, A. V. 2001, AZh, 78, 661 (Engl. transl.: Astron. Rep., 45, 569)

Tverskoy, B. A. 1966, Geomagn. Aeron., 6, 11